Ab Initio Studies of the Reaction of O(^{3}P) with CHClF Radical

Baoshan Wang,* Hua Hou, and Yueshu Gu

School of Chemistry, Shandong University, Jinan, 250100, P. R. China

Received: January 27, 1999; In Final Form: April 7, 1999

The reaction of oxygen atom with chlorofluoromethyl radical has been studied extensively using the G2(MP2) level of theory. The computation reveals an association−elimination mechanism. The addition reaction of O(^{3}P) with CHClF proceeds to the formation of an energy-rich intermediate CHClFO*. Five product channels of CHClFO* are found: Cl + CHFO, H + CClFO, CClFOH, HF + ClCO, and F + CHClO. The isomer CClFOH can decompose through six product channels: H + CClFO, HCl + FCO, HF + ClCO, Cl + FCOH, F + ClCOH, and OH + CFCl (^{1}A′). On the basis of this ab initio potential energy surface, the energy-specific rate constants of the unimolecular decomposition of the activated adduct CHClFO* are used to estimate the branching ratio with RRKM theory. The productions of Cl + CHFO and H + CClFO are shown to be the dominant and competitive reaction channels. The implications of our results are discussed in terms of understanding the atmospheric and combustion chemistry of the CHClF radicals.

I. Introduction

Chlorofluoromethane (HCFC-31, CH_2ClF) is one of the important replacements to the chlorofluorocarbons (CFCs) in many industrial and technological applications. Because CH_2ClF is insoluble in water and volatile in nature, it will eventually escape into the atmosphere. The reaction of CH_2ClF with the hydroxyl radical is thought to be a major source of the CHClF radicals in the troposphere.[1,2] The CHClF radicals then rapidly combine with the oxygen atoms to form chlorofluoromethoxy radicals, which can extrude the Cl atoms easily to take part in the destruction of ozone through the chain reactions, namely,

$$O(^3P) + CHClF \rightarrow CHClFO^*$$
$$CHClFO^* \rightarrow Cl + CHFO$$
$$Cl + O_3 \rightarrow ClO + O_2$$
$$ClO + O(^3P) \rightarrow Cl + O_2$$

Obviously, the studies of the key reaction of O(^{3}P) with CHClF are very valuable in atmospheric chemistry.

The reaction of O(^{3}P) with CHClF radicals is also important in combustion chemistry.[3−5] The incineration of halogenated polymeric wastes produces the rich halogenated methyl radicals such as CHClF. In fuel-lean combustion, the concentrations of oxygen atoms are also relatively high. The reaction of O(^{3}P) with CHClF involves many highly exothermic production channels, viz.:

$$O + CHClF \rightarrow HF + ClCO \quad \Delta H = -114 \text{ kcal/mol}$$
$$\rightarrow HCl + FCO \quad \Delta H = -107 \text{ kcal/mol}$$
$$\rightarrow Cl + CHFO \quad \Delta H = -105 \text{ kcal/mol}$$
$$\rightarrow H + CClFO \quad \Delta H = -94 \text{ kcal/mol}$$
$$\rightarrow F + CHClO \quad \Delta H = -70 \text{ kcal/mol}$$
$$\rightarrow OH + CClF \quad \Delta H = -28 \text{ kcal/mol}$$

All of these channels must play an important role in the combustion process, particularly under high-temperature combustion conditions. Therefore, it is necessary to investigate the reaction mechanism of O + CHClF.

Surprisingly, there is no direct study of the reaction of O + CHClF experimentally and theoretically. Only limited information on the decomposition of the intermediate CHClFO radical is available in the literature. Tuazon et al.[6] reported a 100% yield of CHFO as the primary products, which was attributed to Cl atom elimination from the CHClFO radicals. Using time-resolved mass spectroscopy, Carr et al.[7] observed that the Cl elimination reaction is the dominant process for the decomposition of the CHClFO radicals with a rate of >3000 s^{-1} at 300 K. Rayez et al.[8,9] studied the H, F, and Cl extrusion of CHClFO using the MNDO method. The respective barriers obtained are 29.4, 30.6, and 10.4 kcal/mol, respectively.

We have initiated a systematic study of the reactions of oxygen atom with halogenated methyl. Results of the O + CH_2-Cl and O + CH_2F reactions have been reported elsewhere.[10] In the present work, we report an elaborate study of the reaction of O(^{3}P) with CHClF using ab initio molecular orbital theory. The lowest lying doublet potential energy surface (PES) for this reaction is explored with the G2(MP2) method for the first time. The reaction mechanism is revealed extensively and the kinetic characters are also analyzed on the basis of the present PES. Finally, the implications of our results are discussed in terms of understanding the atmospheric and combustion chemistry of the CHClF radicals.

II. Computation

Ab initio molecular orbital calculations were performed with the Gaussian 94 programs.[11] The geometries of the reactants, products, various intermediates, and transition states were fully optimized at UMP2(full)/6-31G(d) level. The vibrational frequencies were obtained at the same level to determine the nature of different stationary points and the zero-point-energy (ZPE) correction (scaled by 0.93 to eliminate the known systematic errors).[12] All the stationary points have been positively identified for minima with no imaginary frequencies and the transition states with one imaginary frequency. To confirm that the transition states connect between designated reactants and

* Corresponding author. E-mail: guojz@icm.sdu.edu.cn.

10.1021/jp990316x CCC: $18.00
Published on Web 06/11/1999

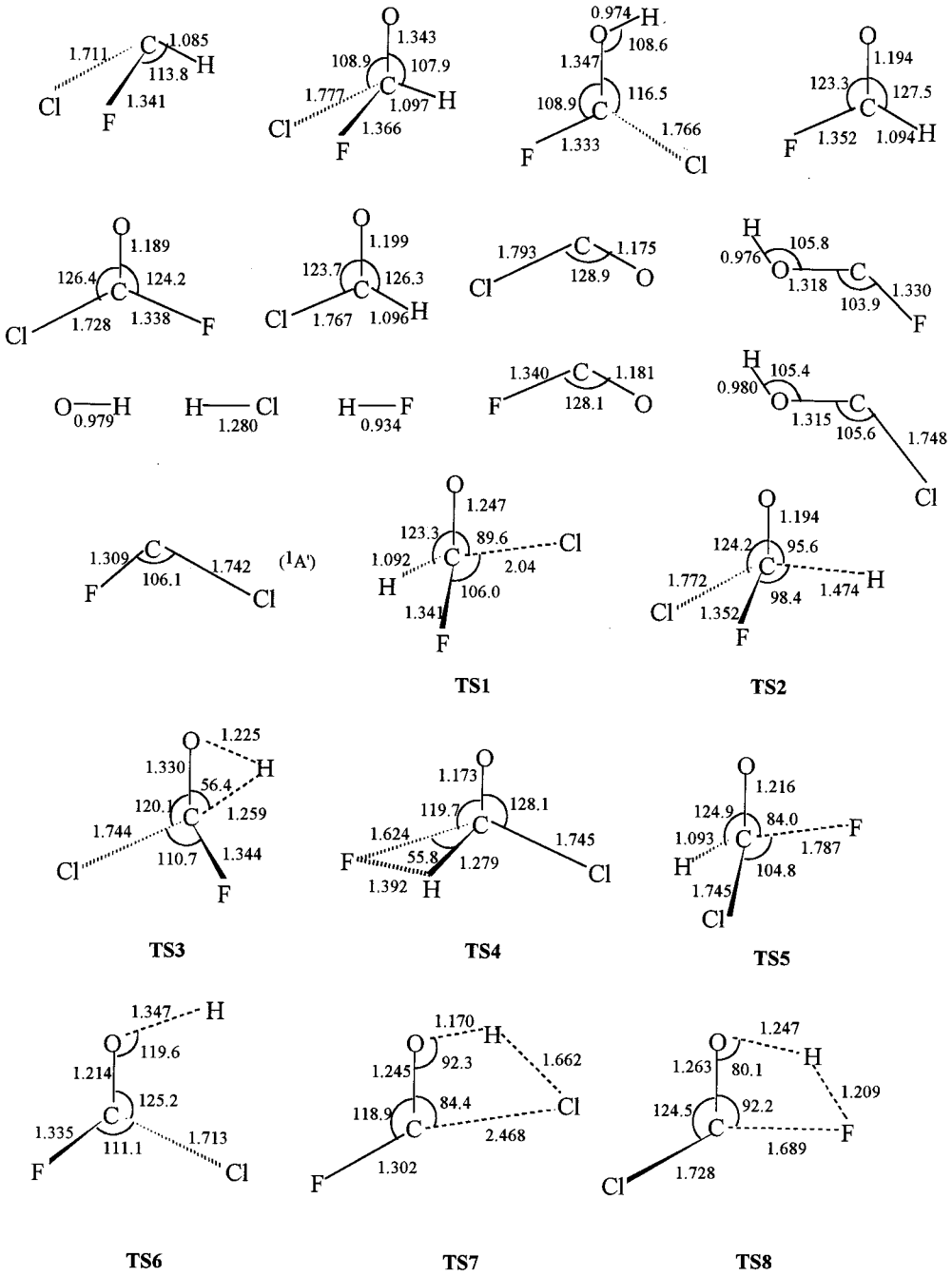

Figure 1. Optimized structures of various species involved in the reaction of $O(^3P)$ with CHClF. Bond distances are in Å, and angles are in degree.

products, we performed also intrinsic reaction coordinate (IRC) calculations[13] at the UMP2(full)/6-31G(d) level. Then the single-point energies were calculated at the UMP2/6-311G(d,p), UMP2/6-311 + G(3df,2p), and QCISD(T)/6-311G(d,p) levels, respectively. Finally, the conventional G2(MP2) scheme[14] was used to obtain the total energies of various species.

III. Results and Discussion

The optimized structures of various species involved in the reaction of $O(^3P)$ with CHClF are shown in Figure 1. The vibrational frequencies are listed in Table 1. The total energies and the relative energies are listed in Table 2. A relaxed attractive potential energy curve for the approach of oxygen atom to the CHClF radical is shown in Figure 2. The profile of the potential energy surface for the reaction of $O(^3P)$ + CHClF is shown in Figure 3 in order to clarify the reaction mechanism.

1. Potential Energy Surface and Reaction Mechanism. Table 2 shows that the calculated reaction heats at 0 K are in quite good agreement with the available experimental data[15,16] within an average deviation of ±1.1 kcal/mol. It implies that the PES obtained at the G2(MP2) level is of high quality. The energetic profile (Figure 3) reveals an association−elimination mechanism for the reaction of $O(^3P)$ with CHClF. As shown in Figure 2, the reaction between two open-shell species, $O(^3P)$ and CHClF, takes place as they are approaching one another to interact on an attractive potential surface. It is obvious that this addition process is barrierless. An intermediate CHClFO (denoted as **IM1**) is formed when the $O(^3P)$ atom combines with the carbon radical center of the CHClF radical. **IM1** belongs to the C_1 point group. The newly formed C−O bond is 1.343 Å. The distances of the C−Cl, C−F, and C−H bonds in **IM1** are somewhat longer than those in the reactant of CHClF.

TABLE 1: Vibrational Frequencies (in cm^{-1}) and Zero-Point Energies (ZPE, in kcal/mol) of the Species Involved in the Reaction of O + CHClF[a]

species	frequencies	ZPE
CHClF	385, 757, 849, 1123, 1273, 3036	10.6
CHFO	616, 978, 1043, 1327, 1755, 2970	12.4
CClFO	390, 473, 626, 717, 1065, 1789	7.23
CHClO	438, 720, 904, 1306, 1684, 2932	11.4
ClCO	356, 603, 1860	4.03
FCO	585, 1020, 1866	4.96
FCOH	613, 721, 1024, 1218, 1304, 3486	12.0
ClCOH	438, 690, 718, 1227, 1242, 3424	11.1
CClF (^{1}A′)	425, 738, 1136	3.28
OH	3478	4.97
HF	3758	5.37
HCl	2835	4.05
IM1	234, 372, 541, 710, 982, 1058, 1171, 1271, 2906	13.2
IM2	307, 380, 392, 560, 708, 1028, 1188, 1294, 3507	13.4
TS1	832i, 258, 327, 599, 895, 1083, 1280, 1376, 2980	12.6
TS2	1758i, 364, 421, 640, 653, 726, 795, 1025, 1702	9.04
TS3	2117i, 356, 403, 568, 634, 723, 1064, 1236, 2398	10.6
TS4	669i, 296, 418, 570, 720, 819, 1183, 1618, 2195	11.2
TS5	1033i, 224, 373, 455, 753, 965, 1319, 1508, 2967	12.2
TS6	2759i, 288, 390, 490, 506, 719, 862, 1111, 1719	8.70
TS7	1710i, 161, 210, 405, 711, 950, 1136, 1475, 1833	9.60
TS8	1680i, 215, 410, 609, 706, 723, 884, 1489, 1886	9.90

[a] i represents imaginary frequency.

TABLE 2: Total Energies (in Hartree) and the Relative Energies (in kcal/mol) of the Species Involved in the Reaction of O + CHClF

species	$\langle S^2\rangle$[a]	G2(MP2)	ΔE	exptl
O + CHClF (C_1)	2.00, 0.76	−673.01410	0.0	
Cl + CHFO (C_s, ^{1}A′)	0.76, 0.0	−673.18587	−107.8	−105
H + CClFO (C_s, ^{1}A′)	0.75, 0.0	−673.16271	−93.2	−94
F + CHClO (C_s, ^{1}A′)	0.75, 0.0	−673.12606	−70.2	−70
HF + ClCO (C_s, ^{2}A′)	0.0, 0.78	−673.19926	−116.2	−114
HCl + FCO (C_s, ^{2}A′)	0.0, 0.78	−673.18972	−110.2	−107
Cl + FCOH (C_s, ^{1}A′)	0.76, 0.0	−673.11814	−65.3	
F + ClCOH (C_s, ^{1}A′)	0.75, 0.0	−673.05302	−24.4	
OH + CClF (C_s, ^{1}A′)	0.76, 0.0	−673.05728	−27.1	−28
IM1 (C_1)	0.76	−673.16734	−96.2	
IM2 (C_1)	0.76	−673.18588	−107.8	
TS1 (C_1)	0.87	−673.16512	−94.8	
TS2 (C_1)	0.86	−673.14341	−81.1	
TS3 (C_1)	0.80	−673.12473	−69.4	
TS4 (C_1)	0.83	−673.11680	−64.4	
TS5 (C_1)	0.93	−673.11572	−63.8	
TS6 (C_1)	0.89	−673.13657	−76.8	
TS7 (C_1)	0.77	−673.13596	−76.5	
TS8 (C_1)	0.76	−673.12112	−67.2	

[a] The expectation value of $\langle S^2\rangle$ before projection. Values after projection are 0.75 for doublet states and 2.00 for triplets. For reactants and products, the first number corresponds to the first species, and the second number corresponds to the second species.

*a. Decomposition of **IM1***. At the G2(MP2) level, the energy of **IM1** is 96.2 kcal/mol lower than that of the reactants O + CHClF. Obviously, the association of O(^{3}P) with CHClF can provide enough energy to make **IM1** highly activated. So **IM1** should be a short-lived hot complex, and can undergo various possible production channels immediately by decomposition or isomerization. Five production channels of **IM1** have been found and will be discussed separately following the energetic sequence.

The energetically most favorable reaction path is **IM1** → Cl + CHFO via C−Cl bond cleavage transition state **TS1**. The barrier height for this channel is only 1.4 kcal/mol. The breaking C−Cl bond is elongated to 2.04 Å with a decrease of the O−C−Cl angle by 20.0°. The C−O bond is shortened by 0.1 Å, forming the final product CHFO. **TS1** appears to be a product-like barrier. The C−Cl bond fission of **IM1** is exothermic by 11.6 kcal/mol, and the overall reaction is also highly exothermic by 107.8 kcal/mol. Therefore, the internal excited product of CHFO should be formed.

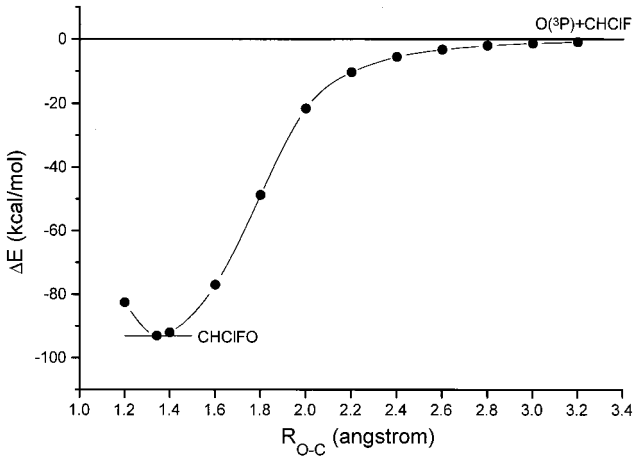

Figure 2. Relaxed potential energy curve for the approach of O(^{3}P) to CHClF radical at the UMP2(full)/6-31G(d) level. The forming O−C bond distance of CHClFO was varied from 1.2 to 3.2 Å with an interval of 0.2 Å; other geometric parameters were optimized for each value of O−C.

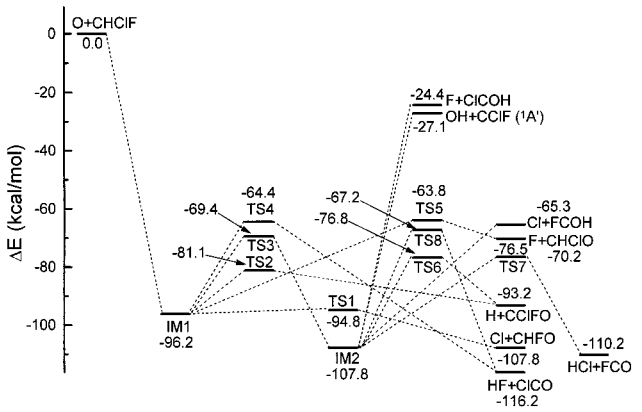

Figure 3. Profile of the potential energy surface for the O(^{3}P) + CHClF reaction at the G2(MP2) level.

The second decomposition pathway of **IM1** produces H atom and CClFO via C−H bond fission transition state **TS2**. The barrier height for this process is 15.1 kcal/mol relative to **IM1**. The breaking C−H bond is elongated from 1.097 Å in **IM1** to 1.474 Å in **TS2**. The C−O bond is shortened by 0.149 Å and is close to that of the final product CClFO. So **TS2** is also a later barrier. Additionally, the barrier is quite narrow due to the large imaginary frequency (1758 cm^{-1}). The C−H dissociation of **IM1** is endothermic by 3.0 kcal/mol. However, the overall reaction (O + CHClF → H + CClFO) is still highly exothermic by 93.2 kcal/mol.

The third reaction channel involves the isomerization of **IM1** via transition state **TS3**. The H atom shifts from the C atom to the O atom, forming an intermediate CClFOH (denoted as **IM2**). The migrating hydrogen is 1.259 Å away from the migrating origin (C) and 1.225 Å from the migrating terminus (O). The calculated barrier height is 26.8 kcal/mol at the G2(MP2) level. The isomer CClFOH has no symmetry. Its energy is 11.6 kcal/mol lower than that of the **IM1**. Therefore, **IM2** possesses the higher internal energy and thus may be more activated. Many decomposition channels of **IM2** would be open as illustrated below.

The fourth possible reaction channel of **IM1** is the 1,1-HF elimination forming HF + ClCO via three-centered transition state **TS4**. As shown in Figure 1, the breaking C−H and C−F bonds are elongated simultaneously by 0.182 Å and 0.258 Å, respectively, with a decrease of the H−C−F angle. The forming H−F bond is 1.392 Å, which is 0.458 Å longer than the equilibrium distance of the HF molecule. The barrier height is as much as 31.8 kcal/mol above **IM1** due to the strong repulsion of the three-membered ring. It is noted that the production of HF + ClCO is the most exothermic channel by 116.2 kcal/mol for the reaction of O + CHClF.

Similar to the reaction of O + CH_2Cl studied previously,[10] the three-center transition state for the production of HCl + FCO from **IM1** cannot be located at the UMP2(full)/6-31G(d) level. Although the C−Cl and C−H bonds are stretched simultaneously with reducing the angle of H−C−Cl to make the distance of the forming H−Cl bond to be various values between 1.28 Å (the equilibrium bond length of HCl) and 2.38 Å (the distance of H−Cl in **IM1**), the resulting stationary structures always are **TS1**, **TS2**, or the H-abstraction transition states for Cl + CHFO and H + CClFO. The higher level calculations (CISD, CCSD, DFT, etc., with the more flexible basis sets) are necessary to check whether this type of HCl elimination three-center transition state exists or not.

The last examined production channel of **IM1** is the formation of F + CHClO via C−F bond fission transition state **TS5**. The breaking C−F bond of 1.787 Å is 0.421 Å longer than that of **IM1**. The C−O bond is shortened by 0.127 Å with reduction of the angle of O−C−F by 24.0°. The barrier height is 32.4 kcal/mol. This C−F bond cleavage of **IM1** is very endothermic by 26.0 kcal/mol, but the overall reaction channel is still exothermic by 70.2 kcal/mol.

When the barriers for H, F, and Cl extrusion of **IM1** of this work at the G2(MP2) level are compared with those reported previously at the MNDO level,[8,9] the differences are −14.3, 1.8, and −9.0 kcal/mol, respectively. It implies that the electron correlation effect must be considered in the study of the O + CHClF reaction.

*b. Decomposition of **IM2**.* As mentioned above, the reaction intermediate CClFOH (**IM2**) can decompose subsequently to various products due to the high internal energy. A total of six production channels of **IM2** are found.

The most feasible decomposition channel of **IM2** is the formation of H and CClFO via O−H bond fission transition state **TS6**. The barrier height for this process is 31.0 kcal/mol relative to **IM2**. The breaking O−H bond is stretched by 0.373 Å, and the C−O bond is shortened by 0.133 Å.

The second decomposition pathway of **IM2** is the 1,2-HCl elimination to form HCl + FCO via a four-membered ring transition state **TS7**. **TS7** is a nearly planar structure. The breaking C−Cl and O−H bonds are 2.468 and 1.170 Å, respectively. The forming H−Cl bond of 1.662 Å is 0.382 Å longer than the equilibrium distance of the HCl molecule. The barrier height is 31.3 kcal/mol relative to **IM2**. It is worthwhile to note that the path O + CHClF → **IM1** → **TS3** → **IM2** → **TS7** → HCl + FCO is the only mechanism to form HCl + FCO in the reaction of O + CHClF we can find at the UMP2-(full)/6-31G(d) level. The overall reaction heat is −110.2 kcal/mol.

Another four-center decomposition of **IM2** produces HF + CClO via transition state **TS8**. The four-membered ring of H−O−C−F is almost planar, while the C−Cl bond is out of the plane. The breaking C−F and O−H bonds are stretched simultaneously by 0.356 and 0.273 Å, respectively. The forming H−F bond is 1.209 Å, which is 0.275 Å longer than the equilibrium distance of the HF molecule. The corresponding barrier height is 40.6 kcal/mol.

The last three reaction channels of **IM2** are all the simple bond fission processes without surmounting the well-defined transition states. The C−Cl, C−F, and C−O bond fissions of **IM2** produce Cl + FCOH, F + ClCOH, and OH + CClF ($^1A'$), respectively. These channels are endothermic relative to **IM2** by 42.5, 83.4, and 80.7 kcal/mol, respectively.

2. Kinetic Analysis. *a. Kinetics of the Overall Reaction*. The O(^{3}P) + CHClF reaction exhibits a typical radical−radical association−elimination mechanism, as can be seen from the energetic profile (Figure 3). The association of O(^{3}P) with CHClF leads to the complex **IM1**, which corresponds to a deep potential well on the PES. Thus, the rate of the redissociation of **IM1** back to the reactants is very slow. On the other hand, the subsequent decomposition reactions of **IM1** occur very fast due to the relatively low exit barriers. Therefore, the barrierless association of O(^{3}P) atom with CHClF radical becomes the rate-limiting step. Similar to the reaction of O + CH_2Cl,[10] the O(^{3}P) + CHClF reaction should have the near gas collisional number rate, i.e., 10^{-10} cm^3 molecule^{-1} s^{-1}. Furthermore, the rate constants should be slightly negative, temperature dependent, and pressure independent because the energy-rich intermediate **IM1** has a relatively short lifetime.

Since the "transition state" for the radical−radical association process of O(^{3}P) with CHClF cannot be obtained through ab initio calculation, the conventional transition state theory (CTST)[17] is not suitable to deduce the rate constants. However, the variational transition state theory (VTST)[18,19] or statistical adiabatic channel model (SACM)[20,21] can effectively treat this reaction. One of the appealing methods is the canonical variational transition state theory (CVTST) developed by Lin et al. recently.[22−27] The maximum free energy of activation ($\Delta G^{\ddagger}$) can be obtained through scanning the relaxed PES, i.e., the potential energy curve (Figure 2), for the approach of O to CHClF. This method has been used to systematically calculate the rate constants of the reactions of O(^{3}P) with halogenated methyl radicals and will be reported separately.

b. Energy-Specific Kinetics. At the lower pressure, the deactivation rate of the energy-rich adduct CHClFO (**IM1**) due to the collisions of the bath gas is relatively slow. The yields of various products in the reaction of O(^{3}P) with CHClF can be estimated by the rates of respective unimolecular decomposition channels of CHClFO, namely,

$$\mathrm{CHClFO} \rightarrow \mathrm{Cl} + \mathrm{CHFO} \quad (1)$$

$$\rightarrow \mathrm{H} + \mathrm{CClFO} \quad (2)$$

$$\rightarrow \mathrm{CClFOH} \quad (3)$$

$$\rightarrow \mathrm{HF} + \mathrm{ClCO} \quad (4)$$

$$\rightarrow \mathrm{F} + \mathrm{CHClO} \quad (5)$$

The energy-specific rate constants are obtained readily by RRKM theory using a simple treatment of adiabatic rotation as[28]

$$k(E) = l_i(I_i/I)^{1/2}G_i(E - E_i^{\ddagger})/hN(E)$$

where l_i is the reaction path degeneracy and h is the Planck's constant. The overall moments of inertia for CHClFO (I) and TS ($I_i^{\ddagger}$) are taken from the present ab initio calculations. $N(E)$ is the density of vibrational state of CHClFO at energy E, $G_i(E - E_i^{\ddagger})$ is the sum of accessible vibrational states of the transition state for channel i at energy $E - E_i^{\ddagger}$, and $E_i^{\ddagger}$ is the corresponding barrier height. Because the transition states for the production

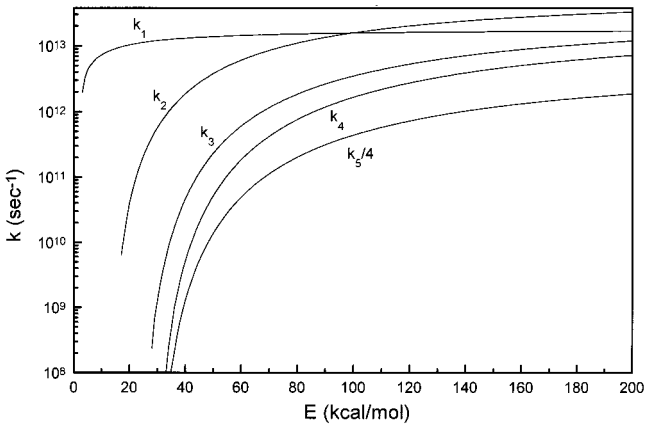

Figure 4. Energy-specific rate constants of five unimolecular decomposition channels of the intermediate CHClFO*. For the sake of clearness, k_5 is divided by a factor of 4.

channels of CHClFO are all tight, $G_i(E - E_i^{\ddagger})$ can be calculated using the Beyer−Swinehart algorithm.[29] $N(E)$ is deduced by the steepest decent method.[28]

The calculated energy-specific rate constants, k_1, k_2, k_3, k_4, and k_5, for five reaction channels as a function of the energy E are depicted in Figure 4. The reaction rate for channel 1, k_1, is much faster at low energies than those for the other four channels due to the lower barrier height for channel 1 (see Figure 3). At energies greater than 100.0 kcal/mol, the reaction rate k_2 for channel 2 begins to exceed k_1 for channel 1 since the vibrational frequencies of **TS2** for channel 2 are smaller than those of **TS1** for channel 1 (see Table 1), which results in a larger sum of states for **TS2**. Within the range of the internal energy considered in this study, k_3, k_4, and k_5 are smaller than k_1 and k_2. k_4 is almost equal to k_5 due to the similar barrier heights and vibrational frequencies.

At $E = E_R$ (E_R is the maximum internal energy that **IM1** can obtain, i.e., 96.2 kcal/mol.), the calculated microcanonical rate constants for these five channels are 1.6×10^{13}, 1.5×10^{13}, 3.2×10^{12}, 1.5×10^{12}, and 1.6×10^{12} (in s^{-1}), respectively. It is obvious that k_1 is equal to k_2 approximately and is larger than the other three rates. Channels 1 and 2 account for 83.1% of the overall yield of the O + CHClF reaction. Thus, the formations of Cl + CHFO and H + CClFO are the dominant and competitive product channels, which is in agreement with the experimental observation.[6,7]

However, it must be noted that the above RRKM calculation is only qualitatively valid. Since the sum of the five rate constants is 3.7×10^{13} s^{-1} at $E = E_R$, the lifetime of **IM1** is only 2.7×10^{-14} s. It is well-known that this lifetime is not long enough to satisfy the statistical basis of RRKM theory, so the strongly bound intermediate in this atom/radical reaction has little effect on the dynamics, which are thus similar to those taking place in a direct process in which no intermediate is possible. The polyatomic product molecules are expected to be born with strongly nonstatistical vibrational distributions.

3. Implication for Atmospheric and Combustion Chemistry. For the CHClF radical, the C−H, C−F, and C−Cl bond dissociation energies are 74, 114, and 74 kcal/mol, respectively.[30] It shows that the CHClF radical is relatively stable. However, when the CHClF radical combines with O atom, the reaction proceeds very fast and, most of all, produces the Cl atom dominantly. So we propose that the reaction of oxygen atom with CHClF will play a key role to the HCFCs involved catalytic destruction of ozone.

On the other hand, it is obvious that most of the highly exothermic product channels of the O + CHClF reaction may contribute significantly to the incineration or combustion chemistry of halogenated polymeric materials over a wide range of temperature. Our goal is to quantify the reaction of O atom with the haloalkyl radicals in order to provide a reliable estimate of their kinetics and dynamics for practical combustion applications.

IV. Conclusions

The reaction of O(^{3}P) with CHClF radical has been examined extensively using the G2(MP2) theory. The calculations reveal a capture-limited association−elimination mechanism. The association of O(^{3}P) with CHClF was found to be a barrierless process forming an energy-rich intermediate CHClFO*. Various decomposition and isomerization reaction channels of CHClFO* were reported. The overall kinetic characters of the O(^{3}P) + CHClF reaction were predicted. The energy-specific rate constants calculated by RRKM theory show that the formations of Cl + CHFO and H + CClFO are the major and competitive production channels. The reaction of O(^{3}P) with CHClF must play an important role in atmospheric and combustion chemistry.

References and Notes

(1) Atkinson, R.; Carter, W. P. L. *J. Atmos. Chem.* **1991**, *13*, 195.
(2) Finlayson-Pitts, B. J.; Pitts, J. N., Jr. *Atmospheric Chemistry: Fundamentals and Experimental Techniques*; John Wiley: New York, 1986.
(3) Senkan, S. M. *Environ. Sci. Technol.* **1988**, *22*, 2368.
(4) Seetula, J. A.; Slagle, I. R.; Gutman, D.; Senkan, S. M. *Chem. Phys. Lett.* **1996**, *252*, 299.
(5) Seetula, J. A.; Slagle, I. R. *Chem. Phys. Lett.* **1997**, *277*, 381.
(6) Tuazon, E. C.; Atkinson, R. *J. Atmos. Chem.* **1993**, *17*, 179.
(7) Bhatnagar, A.; Carr, R. W. *Chem. Phys. Lett.* **1996**, *258*, 651.
(8) Rayez, J. C.; Rayez, M. T.; Halvick, P.; Duguay, B.; Lesclauz, R.; Dannenberg, J. J. *Chem. Phys.* **1987**, *116*, 203.
(9) Rayez, J. C.; Rayez, M. T.; Halvick, P.; Duguay, B.; Dannenberg, J. J. *Chem. Phys.* **1987**, *118*, 265.
(10) Wang, B.; Hou, H.; Gu, Y. *J. Phys. Chem.* **1999**, *103*, 2060.
(11) Frisch, M. J.; Trucks, G. W.; Schlegel, H. B.; Gill, P. W. M.; Johnson, B. G.; Robb, M. A.; Cheeseman, J. R.; Keith, T. A.; Petersson, G. A.; Montgomery, J. A.; Raghavachari, K.; Allaham, M. A.; Zakrzewski, V. G.; Ortiz, J. V.; Foresman, J. B.; Cioslowski, J.; Stefanov, B. B.; Nanayakkara, A.; Challacombe, M.; Peng, C. Y.; Ayala, P. Y.; Chen, W.; Wong, M. W.; Andres, J. L.; Replogle, E. S.; Gomperts, R.; Martin, R. L.; Fox, D. J.; Binkley, J. S.; Defrees, D. J.; Baker, J.; Stewart, J. P.; Head-Gordon, M.; Gonzales, C.; Pople, J. A. *Gaussian 94*; Gaussian Inc.: Pittsburgh, PA, 1995.
(12) Hehre, W. J.; Radom, L.; Schleyer, P. V. R.; Pople, J. A. *Ab initio Molecular Orbital Theory*; John Wiley: New York, 1986.
(13) Gonzalez, C.; Schlegel, H. B. *J. Chem. Phys.* **1989**, *90*, 2154.
(14) Curtiss, L. A.; Ragharachari, K.; Pople, J. A. *J. Chem. Phys.* **1993**, *98*, 1293.
(15) Demore, W. B.; Sander, S. P.; Golden, D. M.; Hampson, R. F.; Kurylo, M. J.; Howard, C. J.; Ravishankara, A. R.; Kolb, C. E.; Molina, M. J. *Chemical Kinetics and Photochemical Data for Use in Stratospheric Modeling*; Evaluation Number 12, 1997.
(16) Boulch, D. L.; Cox, R. A.; Hampson, R. F.; Kerr, J. A., Jr.; Troe, J. *J. Phys. Chem. Ref. Data.* **1980**, *9*, 466.
(17) Smith, I. W. M. *Kinetics and Dynamics of Elementary Gas Reactions*; Butterworth: London, 1980.
(18) Truhlar, D. G. *J. Phys. Chem.* **1979**, *83*, 188.
(19) Truhlar, D. G.; Garrett, B. C. *Acc. Chem. Res.* **1980**, *13*, 440.
(20) Quack, M.; Troe, J. *Ber. Bunsen-Ges. Phys. Chem.* **1974**, *78*, 240.
(21) Quack, M.; Troe, J. *Ber. Bunsen-Ges. Phys. Chem.* **1975**, *79*, 170.
(22) Mebel, A. M.; Morokuma, K.; Lin, M. C. *J. Phys. Chem.* **1995**, *99*, 1900.
(23) Mebel, A. M.; Diau, E. W. G.; Lin, M. C.; Morokuma, K. *J. Am. Chem. Soc.* **1996**, *118*, 9759.
(24) Hsu, C. C.; Lin, M. C.; Mebel, A. M.; Melius, C. F. *J. Phys. Chem.* **1997**, *101*, 60.
(25) Hsu. C. C.; Mebel, A. M.; Lin, M. C. *J. Chem. Phys.* **1996**, *105*, 2346.
(26) ChaKraborty, D.; Park, J.; Lin, M. C. *Chem. Phys.* **1998**, *231*, 29.
(27) Lin, M. C.; He, Y.; Melius, C. F. *J. Phys. Chem.* **1993**, *97*, 9124.
(28) Forst, W. *Theory of Unimolecular Reactions*; Academic Press: New York, 1973.
(29) Stein, S. E.; Rabinovitch, B. S. *J. Chem. Phys.* **1973**, *58*, 2438.
(30) Okabe, H. *Photochemistry of Small Molecules*; John Wiley: New York, 1978.